ANTIOXIDANTS & REDOX SIGNALING
Volume 13, Number 10, 2010

DOI: 10.1089/ars.2010.3137

ORIGINAL RESEARCH COMMUNICATION

Overexpression of Peroxiredoxin 4 Protects Against High-Dose Streptozotocin-Induced Diabetes by Suppressing Oxidative Stress and Cytokines in Transgenic Mice

Yan Ding,[1] Sohsuke Yamada,[1] Ke-Yong Wang,[1] Shohei Shimajiri,[1] Xin Guo,[1] Akihide Tanimoto,[1,2] Yoshitaka Murata,[3] Shuji Kitajima,[4] Teruo Watanabe,[5] Hiroto Izumi,[6] Kimitoshi Kohno,[6] and Yasuyuki Sasaguri[1]

Abstract

Peroxiredoxin 4 (PRDX4) is one of a newly discovered family of antioxidative proteins. We generated human PRDX4 (hPRDX4) transgenic (Tg) mice, displaying a high level of hPRDX4 expression in the pancreatic islets, and then focused on the functions of PRDX4 in a type 1 diabetes mellitus (T1DM) model using a single high dose of streptozotocin (SHDS). After SHDS-injection, Tg mice showed significantly less hyperglycemia and hypoinsulinemia and a much faster response on glucose tolerance test than wild-type (WT) mice. Morphologic and immunohistochemical observation revealed that the pancreatic islet areas of Tg mice were larger along with less CD3-positive lymphocyte infiltration compared with WT mice. Upon comparison between these two mouse models, β-cell apoptosis was also repressed, and reversely, β-cell proliferation was enhanced in Tg mice. Real-time RT-PCR demonstrated that the expression of many inflammatory-related molecules and their receptors and transcription factors were significantly downregulated in Tg mice. These data indicate that PRDX4 can protect pancreatic islet β-cells against injury caused by SHDS-induced insulitis, which strongly suggests that oxidative stress plays an essential role in SHDS-induced diabetes. This study, for the first time, implicates that PRDX4 has a pivotal protective function against diabetes progression in this T1DM model. *Antioxid. Redox Signal.* 13, 1477–1490.

Introduction

Insulin-producing β-cells of pancreatic islets exhibit a markedly low antioxidative defense status and are very susceptible to reactive oxygen species (ROS) such as superoxide anion (O_2^-), hydrogen peroxide (H_2O_2), hydroxyl radicals, and the concomitant generation of nitric oxide (NO) because they have low levels of free radical-detoxifying and redox regulating enzymes, including peroxidases (4, 9, 10, 12). To make matters worse, the alteration of glucose metabolism during type 1 diabetes mellitus (T1DM) progression does not only lead to a corresponding increase in mitochondrial ROS production (10, 12), but also stimulates a dramatic increase in the development of β-cell apoptosis (4, 8, 24). Especially, T1DM models induced by a single high dose of streptozotocin (SHDS) demonstrate a specific disruption of β-cells accompanied by increased ROS production (2).

Toxicity of proinflammatory cytokines, as well as that of oxidative stress, also plays a crucial role in β-cell dysfunction and cell death by apoptosis during the development of T1DM (8, 9, 24). It is known that the majority of T1DM cases can be attributed to autoimmune-mediated specific β-cell apoptosis, which is generally accepted to be an inflammatory disease of the pancreatic islet cells, also known as 'insulitis' (4, 8), quite similar to a delayed type 4 hypersensitivity reaction (8). In fact, β-cell mass is reduced by 70%–80% at the time of diagnosis of T1DM, which reveals that variable degrees of insulitis and even a lack of detectable β-cell apoptosis are present in a stage of diabetes (4, 24), indicating that the progressive depletion of first-phase insulin secretion should start long before

[1]Department of Pathology and Cell Biology, School of Medicine, University of Occupational and Environmental Health, Kitakyushu, Japan.
[2]Department of Tumor Pathology, Field of Oncology, Kagoshima University Graduate School of Medical and Dental Sciences, Kagoshima, Japan.
[3]Kyurin Omtest Laboratory Department, Kyurin Corp., Kitakyushu, Japan.
[4]Analytical Research Center for Experimental Sciences, Saga University, Saga, Japan.
[5]Laboratory of Pathology, Fukuoka Wajiro Hospital, Fukuoka, Japan.
[6]Department of Molecular Biology, School of Medicine, University of Occupational and Environmental Health, Kitakyushu, Japan.

the development of T1DM. Apoptosis of β-cells in insulitis can be caused either by direct contact with activated T-cells and macrophages or by exposure to soluble inflammatory mediators secreted by these cells (8, 24). Indeed, emerging reports show the expression of proinflammatory cytokines in the pancreas of T1DM (1, 2, 28).

A newly discovered family of antioxidative proteins, now designated as peroxiredoxin (PRDX), is ubiquitously synthesized and abundantly identified in various organisms (30). The PRDX family, which includes at least six distinct PRDX genes expressed in mammals, contains a reactive Cys in a conserved region near the N-terminus that forms cysteine-sulfenic acid as a reaction intermediate during the reduction of peroxide, and functional peroxidase activity is dependent on reduced forms of thioredoxin and/or glutathione (19, 30). The function of PRDXs, however, still remains unclear, even though several studies have shown that PRDXs suppress downstream signaling mediated by various types of receptors, such as the signaling of apoptosis (19, 28). *In vivo*, PRDX1 prevents excessive endothelial activation and atherosclerosis (14), and PRDX1 deficiency increases the susceptibility to multiple cancers with aging (26). Loss of PRDX2 is sufficient to influence the growth and migration of smooth muscle cells during vascular remodeling (3). These data show PRDX may not function only in an antioxidative signaling but also in other protective cascades against various types of pathological processes.

Human PRDX4 (hPRDX4) was first identified by yeast 2-hybrid screening as a partner for a thiol-specific antioxidant (11), and in contrast to the intracellular localization of other family members, it is the only known secretory form located in the extracellular space (25, 30), and exerts its protective function against oxidative damage by scavenging ROS in the extracellular space (18, 25). However, despite the regulatory role of PRDX4 in the nuclear factor κB (NF-κB) (18), epidermal growth factor, and p53 (37) or thromboxane A2 receptor (11) cascade shown in several previous studies, the pathological and physiological relevance of PRDX4 remains to be clarified. To investigate the aggravation of T1DM by increasing oxidative stress and the protective function of PRDX4 against insulitis, we generated hPRDX4 transgenic (Tg) mice and evaluated the role of PRDX4 in a T1DM model induced by SHDS.

Materials and Methods

Construction of human PRDX4 transgenic mice

Tg mice were generated using the following procedure. hPRDX4 cDNA was amplified by reverse transcriptase-polymerase chain reaction (RT-PCR) and cloned into the pGEM-T easy vector system (Invitrogen, Life Technologies Japan Ltd., Tokyo, Japan) (Fig. 1A), and its primers were based on a published sequence (Genebank accession no. NM_006406). The *Not*I fragment containing hPRDX4 cDNA was inserted into the *Not*I site of 5.4 Kb pcDNA3 (Invitrogen), and a bovine growth hormone polyadenylation (BGHPA) sequence was inserted into the tail of transgene to stabilize the expression. The entire nucleic acid sequence, containing a 0.6 Kb cytomegalovirus (CMV) enhancer/promoter, 0.8 Kb hPRDX4 cDNA, and 0.2 Kb BGHPA, was purified by restriction enzyme digestion with *Bgl*II and *Sma*I, and was microinjected into male pronuclei of one-cell C57BL/6 mouse embryos with standard transgenic technology. However, this CMV promoter is not a tissue-specific promoter, suggesting that the expression of hPRDX4 transgene at protein levels will be affected by the integration site of mouse genome. C57BL/6 mice (Charles River Laboratories, Yokohama, Japan) were used as the control wild-type (WT) mice in this study.

Animals and type 1 diabetes mouse model

Experiments were performed on 8-week-old male WT and Tg mice weighing 20–25 g. Mice were fasted for 18 h and intraperitoneally injected with a SHDS (Sigma-Aldrich, Co., St Louis, MO) at 150 mg/kg body weight, dissolved in sodium citrate buffer (pH 4.5). The third day after SHDS-injection, blood glucose was measured from blood obtained from the mice tail veins using a blood glucose monitor (Sanwa Kagaku Kenkyusho CO., Ltd. Nagoya, Japan), and mice with blood glucose levels higher than 250 mg/dl were considered to be diabetic. Controls were given the same volume of sodium citrate buffer. Animals were killed 1 or 2 weeks (wk) after SHDS-injection by intraperitoneal anesthetization with an overdose of ketamine and medetomidine, and the pancreases were excised.

Serving as the other protocol of multiple low-dose streptozotocin (MLDS)-induced T1DM, mice were treated with intraperitoneal injections of STZ (40 mg/kg body weight) during 5 consecutive days; day 1 was defined as the day of the first injection of streptozotocin. Blood glucose concentrations were measured on days 0, 3, 7, 14, and 21.

All protocols were approved by the Ethics Committee of Animal Care and Experimentation, University of Occupational and Environmental Health, Japan, and were performed according to the Institutional Guidelines for Animal Experiments and the Law (no. 105) and Notification (no. 6) of the Japanese Government.

Histology and immunohistochemistry

We studied more than 10 animals from each group investigated. The pancreatic tissues were removed and immediately immersed in cold PBS, fixed in 10% neutral buffered formalin, and embedded in paraffin. Paraffin sections (4 μm) were prepared for hematoxylin and eosin (H&E) or immunohistochemical staining. For detection of hPRDX4, a rabbit anti-human polyclonal antibody (1:500; Affinity BioReagents, Golden, CO) was used. To analyze the alterations of islet areas before and after SHDS-injection, images of H&E sections were captured and areas were calculated using a NanoZoomer Digital Pathology Virtual Slide Viewer soft (Hamamatsu Photonics Corp., Hamamatsu, Japan). To evaluate the expression of insulin and glucagon, we performed immunohistochemistry using a guinea pig anti-porcine polyclonal insulin antibody (1:200; DAKO Corporation, Carpinteria, CA) and a rabbit anti-human polyclonal glucagon antibody (1:1; DAKO Cytomation Co., Kyoto, Japan). Additionally, double immunostaining was performed to detect the distribution of both insulin- and glucagon-positive cells among the islets (glucagon with Vulcan Fast Red and insulin with DAB as a substrate, respectively) using the MACH 2 Double Stain system (BIOCARE MEDICAL, LLC., Concord, CA). To detect either hPRDX4- and insulin-positive β-cells or both hPRDX4- and glucagon-positive α-cells in islets, we performed hPRDX4

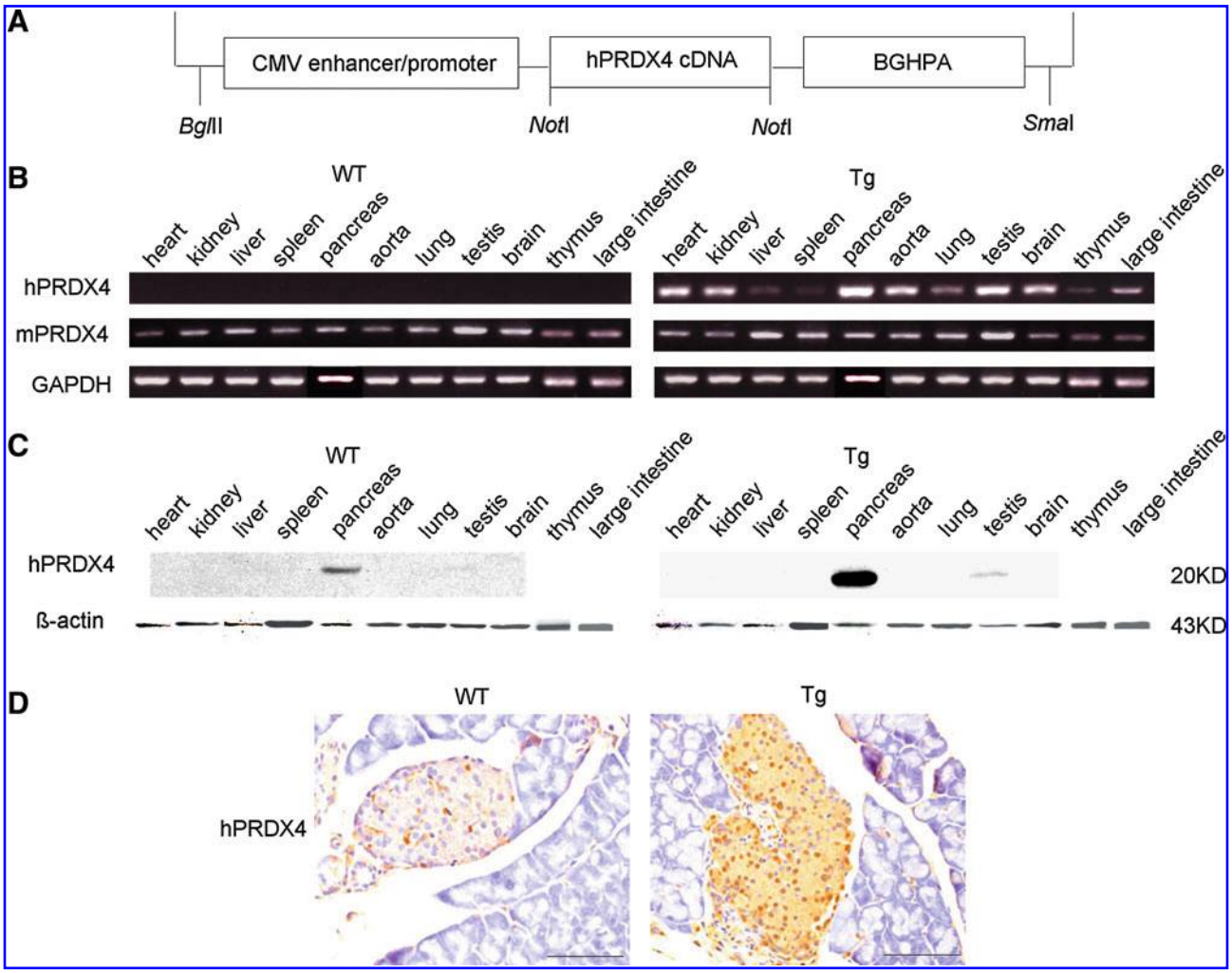

FIG. 1. Schema of human peroxiredoxin 4 (hPRDX4) transgene construct and the expression of hPRDX4 in WT and Tg mice. (**A**) hPRDX4 cDNA (0.8 Kb) was driven by the cytomegalovirus (CMV) enhancer/promoter (0.6 Kb). A bovine growth hormone (BGH) polyadenylation (polyA) sequence (0.2 Kb) was inserted into the transgene to stabilize the expression. The construct was purified from the pcDNA3 (5.4 Kb) by restriction digestion with *Bgl*II and *Sma*I. (**B**) In RT-PCR, Tg mice expressed hPRDX4 mRNA in every tissue, which was more markedly expressed in pancreas, heart, aorta, testis, and brain. No expression was observed in WT mice. The expression of mPRDX4 was clearly recognized in every tissue of nontreated mice, and in particular, was observed in the pancreas, testis, liver, and brain. (**C**) In Western blotting, hPRDX4 was markedly expressed in nontreated Tg pancreas, and to a lesser amount, in nontreated Tg testis. In addition, nontreated WT pancreas showed a faint expression of hPRDX4. (**D**) In immunohistochemistry, hPRDX4 was expressed particularly in Tg pancreatic islets, ductal epithelium, and a small number of acinar cells. (**D**) 200X, $Bar = 100\,\mu$m. (For interpretation of the references to color in this figure legend, the reader is referred to the web version of this article at www.liebertonline.com/ars).

and insulin or glucagon staining on sequential sections and captured the mirror images. For analysis of ROS/oxidative stress expression in pancreas before and after SHDS-injection, we used an anti-8-hydroxy-2′-deoxyguanosine (8-OHdG) monoclonal antibody (1:100; Japan Institute for the Control of Aging, Fukuroi, Japan) (15, 21). To determine the SHDS-induced insulitis, a polyclonal rabbit anti-human CD3 antibody (1:1; DAKO Cytomation Co.) or an anti-mouse Mac-2 monoclonal antibody (1:500; Cedarlane Laboratories Ltd., Burlington, Ontario, Canada) was used, and we counted positive T-cells or macrophages in one islet. Additionally, caspase-3 (1:25; Epitomics, Inc., Burlingame, CA) and MIB-1 (1:2000; Epitomics, Inc.) rabbit monoclonal antibodies were used to analyze β-cells apoptotic activity and the degree of β-cells proliferation, respectively.

Reverse transcriptase-polymerase chain reaction

To assess the expression of the hPRDX4 transgene, total RNA isolated from various tissues using Trizol reagent (Invitrogen) was analyzed by RT-PCR. The relative amounts of PCR products were normalized by those of mGAPDH. The pairs of primers specific for hPRDX4, mGAPDH and mouse PRDX4 (mPRDX4) are shown in Supplement 1 (*see* www.liebertonline.com/ars).

Western blotting analysis

Proteins (40 μg) isolated from WT and Tg mice tissues were separated by electrophoresis on 10% SDS-PAGE gels and transferred onto Immun-Blot PVDF membranes (Bio-Rad

Laboratories, K.K., Tokyo, Japan). The membranes were incubated with a rabbit anti-human polyclonal hPRDX4 antibody (1:10,000) and a mouse anti-chicken monoclonal β-actin antibody (1:1000; Santa Cruz Biotechnology, Inc., Santa Cruz, CA).

ELISA for insulin

The concentration of serum insulin on days 0, 3, 7, and 14 after SHDS-injection was measured using an ELISA kit (Morinaga Institute of Biological Science, Inc., Yokohama, Japan).

Glucose tolerance and glucose response test

To determine glucose tolerance, mice were fasted for 18 h and given an intraperitoneal injection of glucose (1 mg/g body weight). For the glucose response to insulin injection, mice received an intraperitoneal injection of insulin at a dose of 1 U/kg body weight. Both blood samples were withdrawn from the tail vein promptly at 0, 30, 60, and 120 min after injection.

Real-time PCR

After cDNA was synthesized, quantitative real-time PCR was performed using a TaqMan fluorogenic probe method with an ABI PRISM 7000 (Applied Biosystems, Foster City, CA). The pairs of specific primers and probes are shown in Supplement 2 (*see* www.liebertonline.com/ars). The relative amounts of the gene expression were normalized by that of 18S ribosomal RNA (rRNA) using random primers.

TUNEL analysis

To measure the percentage of β-cells apoptosis, TUNEL assays were performed using TACS™ 2 TdT-DAB *in situ* Apoptosis Detection Kit (Trevigen, Inc., Gaithersburg, MD) on pancreatic paraffin sections.

Statistical analysis

Results were expressed as means $\pm$ SE. Significant differences were analyzed using the Student's or Welch's *t*-test or ANOVA analysis where appropriate. A value of $p < 0.05$ was considered to be statistically significant.

Results

Expression of PRDX4 gene and its influence on glucose homeostasis

The expression of hPRDX4 mRNA and protein in various tissues of nontreated Tg and WT mice was detected by RT- and real-time RT-PCR and Western blotting. In PCR, the expression of mPRDX4 was clearly recognized in every tissue of nontreated mice, and in particular, was observed in the pancreas, testis, liver, and brain. The hPRDX4 expression in Tg mice was highly enhanced in the pancreas, heart, aorta, testis, and brain (Fig. 1B). Western blotting analysis (Fig. 1C) revealed that hPRDX4 was markedly expressed in nontreated Tg pancreas, and to a lesser amount, in the testis, whereas nontreated WT pancreas showed a faint band reactive for the anti-hPRDX4 antibody, indicating a slight cross-reaction of the antibody to mPRDX4. Immunohistochemistry showed hPRDX4 was expressed particularly in non-treated Tg islets including β- and α-cells (Supplemental Fig. 1; *see* www.liebertonline.com/ars), ductal epithelium, and a small number of acinar cells (Fig. 1D), but was not expressed in nontreated WT mice. Additionally, immunohistochemical results showed that a small number of spermatogenic cells only from the testis of Tg mice were specifically positive for hPRDX4 (Supplemental Fig. 2, *see* www.liebertonline.com/ars). However, no morphological or biochemical difference was seen between the testes of the two groups of mice (data not shown). Smooth muscle cells in the Tg aorta and columnar epithelial cells in the Tg large intestine also revealed a weak expression of hPRDX4 by immunohistochemistry (Supplemental Fig. 2), but this data was inconsistent with the Western blotting findings that showed no band of hPRDX4 (Fig. 1C). On the other hand, the other Tg tissues, including hypothalamus, thymus, or spleen (Supplemental Fig. 2), and all WT tissues (data not shown) displayed no expression for hPRDX4 in immunohistochemistry.

The pancreatic islet area from nontreated WT and Tg mice showed no difference (WT $24.0 \pm 1.9 \times 10^3$ μm^2 vs. Tg $24.9 \pm 2.5 \times 10^3$ μm^2) (Fig. 2A), and the percentage of insulin-positive cells in nontreated WT islet was very similar to that of Tg mice (WT $87.5 \pm 2.0\%$ vs. Tg $85.9 \pm 1.3\%$) (Fig. 2B).

Next, on the glucose tolerance test, glucose levels were found to be maximal 30 min after glucose injection (Fig. 2C). However, there was no significant difference between nontreated WT and Tg mice at 30, 60, or 120 min. In addition, the result of the glucose response test also did not show any significant difference at any time between the two groups (Fig. 2D).

The contrast of metabolic parameters between WT and Tg mice after SHDS- or MLDS-injection

Blood glucose was detected on days 3, 7, and 14 after SHDS-injection. All treated animals developed hyperglycemia as a model of diabetes, while blood glucose in Tg mice demonstrated a slower increase and less hyperglycemia than that of WT mice for 1 and 2 wk ($p < 0.05$; Fig. 3A). The insulin levels of serum, measured by ELISA, quickly decreased in both groups, and were not significantly different between the two on days 0 and 3 after SHDS-treatment. However, insulin synthesis was significantly increased in Tg mice 1 (WT 69.2 ± 17.5 pg/ml vs. Tg 123.4 ± 17.4 pg/ml) and 2 wk (WT 91.7 ± 14.8 pg/ml vs. Tg 292.7 ± 82.9 pg/ml) after SHDS-injection compared with that of WT mice ($p < 0.05$; Fig. 3B). Furthermore, the body weight of treated WT mice was significantly less than that of Tg mice at 2 wk ($p < 0.05$; data not shown).

Although basal blood glucose levels after fasting were not different between the two groups, after glucose injection, the normalization of increased blood glucose in Tg mice was faster than that of WT mice ($p < 0.05$; Fig. 3C). Blood glucose concentrations after insulin injection showed a lower tendency in Tg mice compared with WT mice, but this difference was not significant between the two groups at 0, 30, 60, 120 min (Fig. 3D).

Whereas, the blood glucose concentrations increased in both WT and Tg mice on day 14 and 21 after given a MLDS-injection, no significant differences were found between two groups on day 0, 3, 7, 14, and 21, respectively (Supplemental Fig. 3A; *see* www.liebertonline.com/ars).

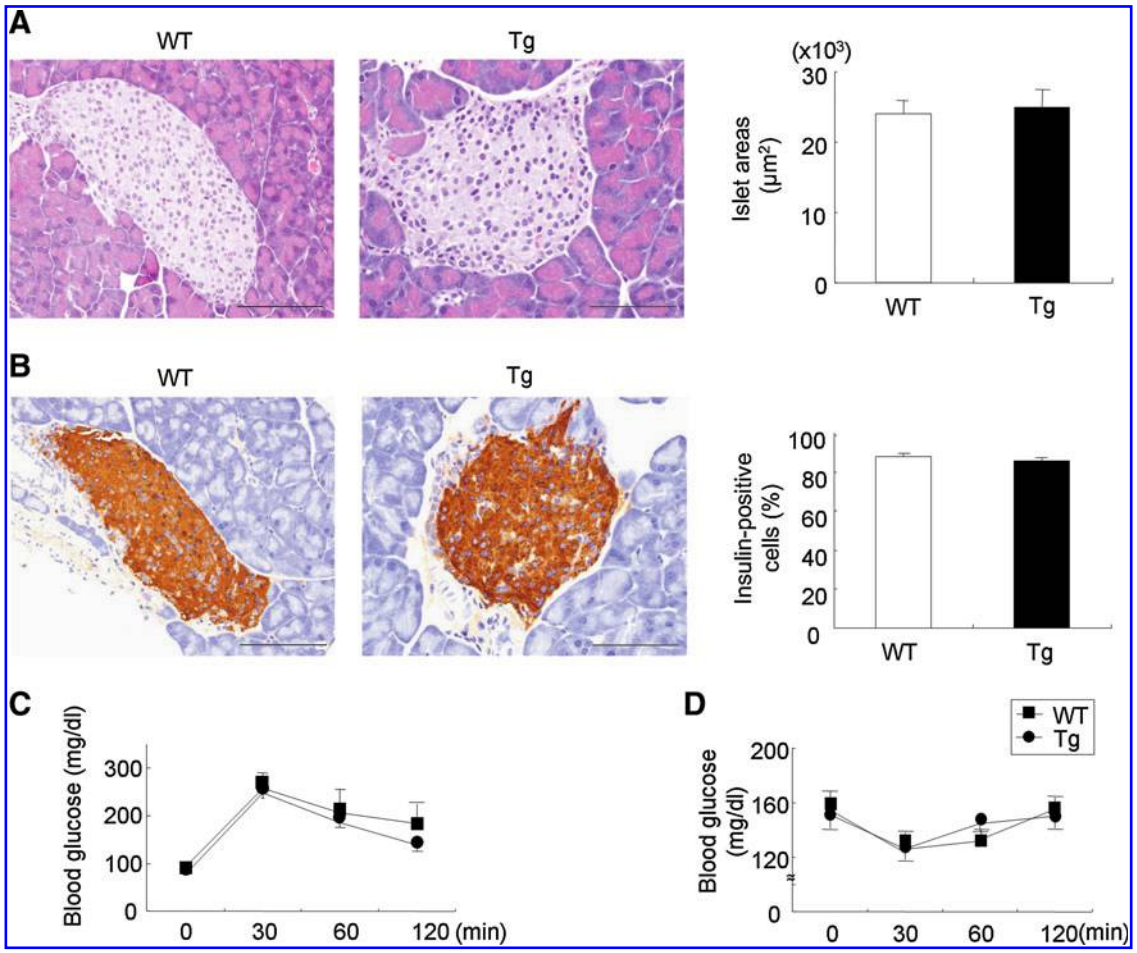

FIG. 2. Expression of hPRDX4 does not affect islet histology and glucose homeostasis in WT and Tg mice under basal conditions. (**A**) Pancreatic islet area revealed no difference between nontreated WT ($24.0 \pm 1.9 \times 10^3$ μm^2) and Tg pancreas ($24.9 \pm 2.5 \times 10^3$ μm^2). (**B**) Immunohistochemical analysis showed that the cellular components of insulin-positive cells in WT islets ($87.5 \pm 2.0\%$) were very similar to those of Tg islets ($85.9 \pm 1.3\%$). (**C**) Glucose tolerance and (**D**) glucose response test showed no significant difference between WT and Tg mice before and at 30, 60, and 120 min after intraperitoneal glucose (**C**) or insulin (**D**) injection. (**A**) and (**B**) 200X, *Bar* = 100 μm. (For interpretation of the references to color in this figure legend, the reader is referred to the web version of this article at www.liebertonline.com/ars).

Alterations of islet areas and hPRDX4 or mPRDXs expression induced by SHDS- and MDLS-injection in WT and Tg pancreas

In H&E staining, islet areas of both WT and Tg mice were markedly decreased compared with those of untreated controls, and the area of islets were not different between WT and Tg mice 1 wk after SHDS-injection (WT $5.8 \pm 0.5 \times 10^3$ μm^2 vs. Tg $6.3 \pm 0.5 \times 10^3$ μm^2). The islet area of WT mice continuously decreased during the 2 wk after SHDS-injection ($p < 0.05$), whereas Tg islet area significantly recovered at 2 wk ($9.2 \pm 0.8 \times 10^3$ μm^2) compared with that of 1 wk ($p < 0.05$), and was 2.2-fold larger than that of WT mice at 2 wk ($4.2 \pm 0.4 \times 10^3$ μm^2) ($p < 0.0001$; Figs. 4A and 4B).

At 3 wk after MLDS injection, islet areas demonstrated no significant difference between WT and Tg mice (WT $3.3 \pm 0.7 \times 10^3$ μm^2 vs. Tg $3.6 \pm 0.5 \times 10^3 \mu m^2$) (Supplemental Fig. 3B).

In addition, immunohistochemistry and real-time PCR demonstrated little or no expression of hPRDX4 in WT mice, whereas high expression of this peroxiredoxin remained in Tg islets both 1 and 2 wk after SHDS-injection (Figs. 4C and 4D). Similar to the results of the basal condition, not only both hPRDX4- and insulin-positive β-cells, but also both hPRDX4- and glucagon-positive α-cells were easily detected at 1 and 2 wks by mirror images of immunostained sequential sections (Supplemental Fig. 1). Additionally, we also exhibited the expression of mPRDX4 in WT and Tg mice pancreas at 0, 1, and 2 wk after SHDS-injection by RT- and real time-PCR. The results revealed that although no difference was noted under basal conditions between WT and Tg mice, the mPRDX4 expressions in Tg pancreas were significantly higher than those in WT mice at 1 and 2 wk after SHDS-injection (Fig. 5A). In addition, the other endogenous isoforms including mPRDX1, 2, 3, 5, and 6 demonstrated similar expressions (Fig. 5B).

Loss of β-cells and insulitis in islets induced by SHDS- or MLDS-injection

Immunohistochemistry showed that insulin-positive β-cells diminished in both WT and Tg islets 2 wk after

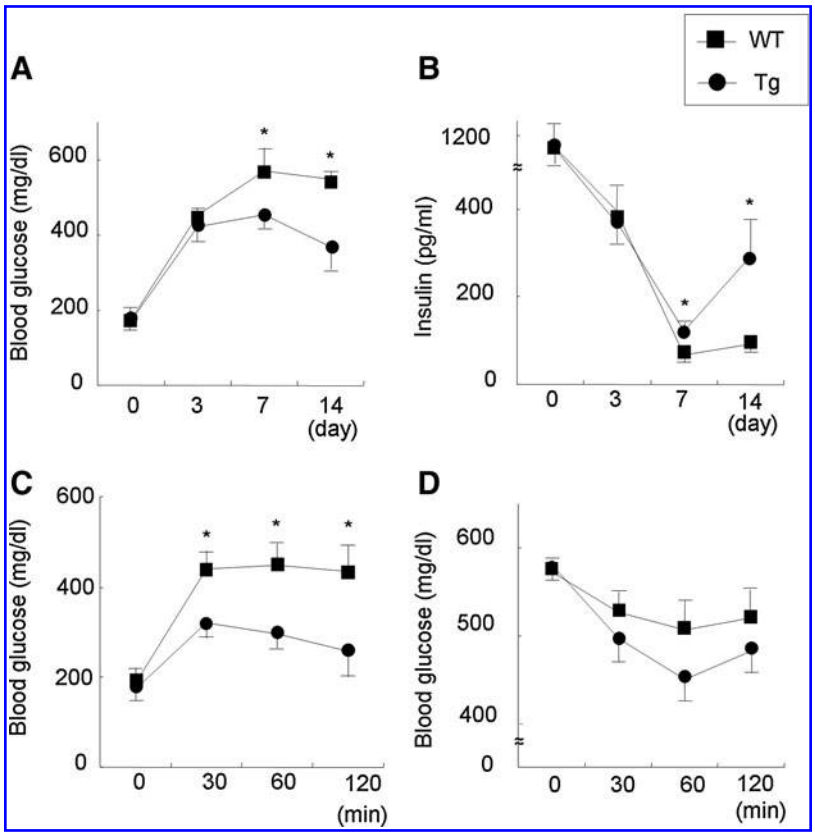

FIG. 3. Comparison of metabolic parameters between WT and Tg mice after SHDS-injection. (**A**) All animals developed hyperglycemia as a model of diabetes after SHDS-injection beginning on day 3, while the blood glucose in Tg mice demonstrated a slower increase and less hyperglycemia than that of WT mice on day 7 and 14, respectively. (**B**) ELISA for insulin. Both WT and Tg mice insulin levels quickly decreased after SHDS-injection compared with controls, and insulin concentration showed no significant difference between WT and Tg mice on day 0 and 3. However, synthesized insulin demonstrated significantly increased levels in Tg compared with that of WT mice on day 7 (WT 69.2 ± 17.5 pg/ml vs. Tg 123.4 ± 17.4 pg/ml) and day 14 (WT 91.7 ± 14.8 pg/ml vs. Tg 292.7 ± 82.9 pg/ml) after SHDS-injection. (**C**) Glucose tolerance test. After glucose injection, both WT and Tg mice blood glucose concentrations increased immediately by 30 min. However, the normalization of blood glucose in Tg mice was significantly faster than that of WT mice. (**D**) Glucose response test. Blood glucose level showed no significant difference in WT and Tg mice after insulin injection. $^*p < 0.05$.

SHDS-injection (Fig. 6A) compared with those of controls. The percentage of β-cells in one islet, however, was significantly higher in Tg than WT mice after SHDS-injection (WT $27.8 \pm 1.5\%$ vs. Tg $41.8 \pm 2.5\%$; $p < 0.0001$), but there was no difference in glucagon-positive α-cells (Fig. 6B) (WT $63.0 \pm 1.6\%$ vs. Tg $64.6 \pm 1.5\%$). Double immunostaining for both insulin (brown)- and glucagon (red)-positive cells was specifically noted only in Tg islets (Fig. 6C).

CD3-staining demonstrated that in all animals insulitis appeared 2 wk after SHDS-injection (see Fig. 10A), but Tg mice showed a lesser number of infiltrating lymphocytes than that of WT mice (WT 10.1 ± 0.7 vs. Tg 6.6 ± 0.4; $p < 0.0001$). Mac-2-staining showed that the number of macrophages per islet exhibited no difference between the two groups (WT 8.0 ± 0.4 vs. Tg 7.5 ± 0.5) (Fig.10B).

As to MLDS models, the percentage of insulin-positive β-cells per islet also demonstrated no significant difference between WT and Tg mice at 3 wk after MLDSinjection (WT $25.7 \pm 2.3\%$ vs. $26.7 \pm 1.7\%$) (Supplemental Fig. 3C).

Levels of 8-OHdG in WT and Tg islets before and after SHDS -injection

We detected the expression of 8-OHdG, a marker for oxidative stress, using immunohistochemistry (Fig. 7). The percentage of 8-OHdG-positive cells in per islet was very low in both untreated WT and Tg mice (WT $2.2 \pm 0.3\%$ vs. Tg $2.3 \pm 0.4\%$, data not shown), whereas after SHDS injection, those expressions in both groups were significantly increased. Although a p value of 0.063 can be considered to be borderline (in)significant between two groups, 8-OHdG expression was suppressed in Tg mice as compared with that in WT mice at 2 wk (WT $86.4 \pm 1.4\%$ vs. Tg $81.6 \pm 2.4\%$, data not shown).

Analysis of inflammatory signaling and tissue remodeling in WT and Tg pancreas

Real-time RT-PCR demonstrated that various genes including interleukin (IL)-1β, tumor necrosis factor (TNF)-α, tumor necrosis factor receptor (TNFR)2, Toll-like receptor (TLR)3/4, and NF-κB were markedly increased in WT mice 2 wk after SHDS-injection compared with untreated WT and treated Tg mice ($p < 0.05$; Fig. 8). These genes, however, did not show such an upregulation in Tg mice except for IL-1β compared with the untreated Tg mice ($p < 0.05$). In addition to these genes, the expression of signal transducer and activator of transcription-1 (STAT1) was significantly downregulated in Tg mice compared with both those of treated and untreated WT mice ($p < 0.05$). Changes in the expression of TLR2 (Fig. 8), IL-1R1, interferon (IFN)-γ, and inducible nitric oxide synthase (iNOS) (data not shown) were not detected in these animals.

Analysis of β-cells apoptosis and proliferation

Although a small number of apoptotic β-cells were observed in both WT and Tg islets 1 wk after SHDS-injection, the percentage of TUNEL-positive cells was much lower in Tg ($1.0 \pm 0.6\%$) than in WT mice ($3.2 \pm 0.7\%$) ($p < 0.05$; Fig. 9A). Similar to TUNEL results, caspase-3-positive cells demonstrated a significant decrease in Tg mice ($2.7 \pm 1.2\%$) compared with WT mice ($9.7 \pm 3.2\%$) ($p < 0.05$; Fig. 9B). Furthermore, the percentage of MIB-1-positive cells significantly increased in Tg

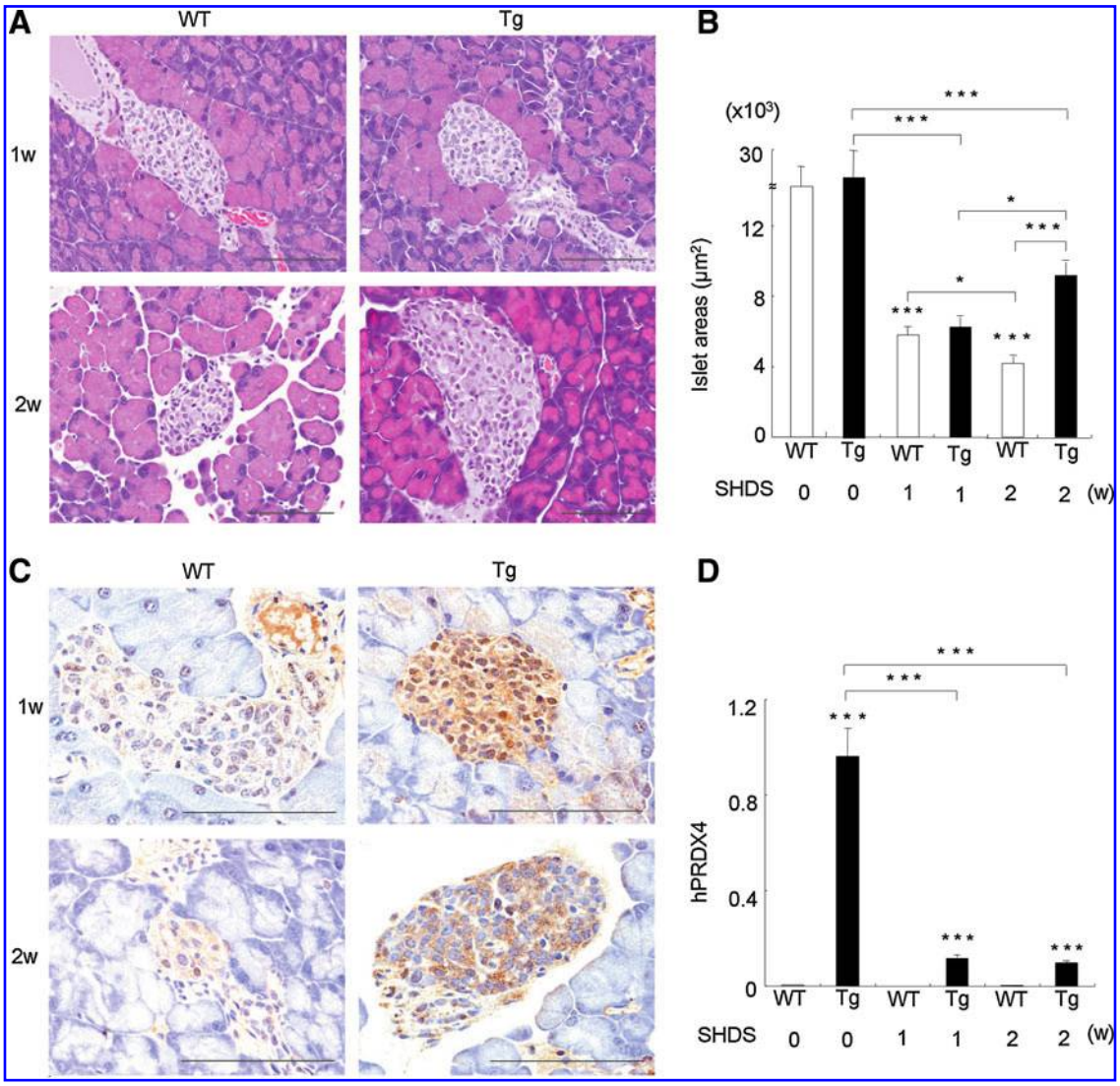

FIG. 4. Alterations of islet areas and hPRDX4 expression in WT and Tg pancreas after SHDS-injection. (**A**) and (**B**) Pancreatic islet area showed no significant difference in WT and Tg mice at 1 wk after SHDS -injection (WT $5.8 \pm 0.5 \times 10^3$ μm^2 vs. Tg $6.3 \pm 0.5 \times 10^3$ μm^2). WT islet area continuously decreased during the first 2 wk, whereas Tg islet area significantly recovered at 2 wk ($9.2 \pm 0.8 \times 10^3$ μm^2) compared with that of 1 wk after SHDS-injection. Therefore, Tg islet area was significantly larger by 2.2-fold than that of WT ($4.2 \pm 0.4 \times 10^3$ μm^2) 2 wk after SHDS-treatment. (**C**) In immunohistochemistry, there was little or no expression of hPRDX4 in WT islets, whereas Tg islets expressed a much higher level of that after SHDS-injection 1 and 2 wk. (**D**) In real-time PCR, hPRDX4 was observed specifically in Tg pancreas during the 2 wk, and its expression decreased 1 or 2 wk after SHDS-injection. (**A**) 200X, (**C**) 400X, *Bar* = 100 μm. *$p < 0.05$, ***$p < 0.0001$.

islets at wk 1 ($13.9 \pm 0.9\%$) compared with that of WT islets ($8.7 \pm 0.6\%$) ($p < 0.0001$; Fig. 9C).

MMPs analysis

The analysis of MMPs demonstrated that MMP2, 3, 7, and 9 were significantly upregulated in WT pancreas compared with those of Tg mice treated for 2 wk and untreated WT mice ($p < 0.05$; Fig. 10C). Only MMP7 expression was higher in Tg mice than that of untreated mice.

Discussion

In the current study, Tg mice exhibited a relatively specific and high expression of hPRDX4 in islets of the pancreas, which were verified by real-time RT-PCR or by immunohistochemistry, respectively (Fig. 1). PRDX4 is the only known secretory form located in the extracellular space (18, 25, 30) such as in the vascular vessels ranging from small to large sizes, where atherosclerotic lesions are called arteriolosclerosis to atheroma. Additionally, as to the former "arteriolosclerosis", diabetes is closely related to its pathophysiological features. Therefore, we hypothesized that this unique PRDX4 *in vivo* plays a pivotal role in the protection against the autoimmune destruction of pancreatic β-cells during the development of diabetes, with a T1DM model induced by SHDS-injection. Morphological and biochemical examinations between WT and Tg mice showed no difference in endogenous mPRDX4 expression, pancreatic islet

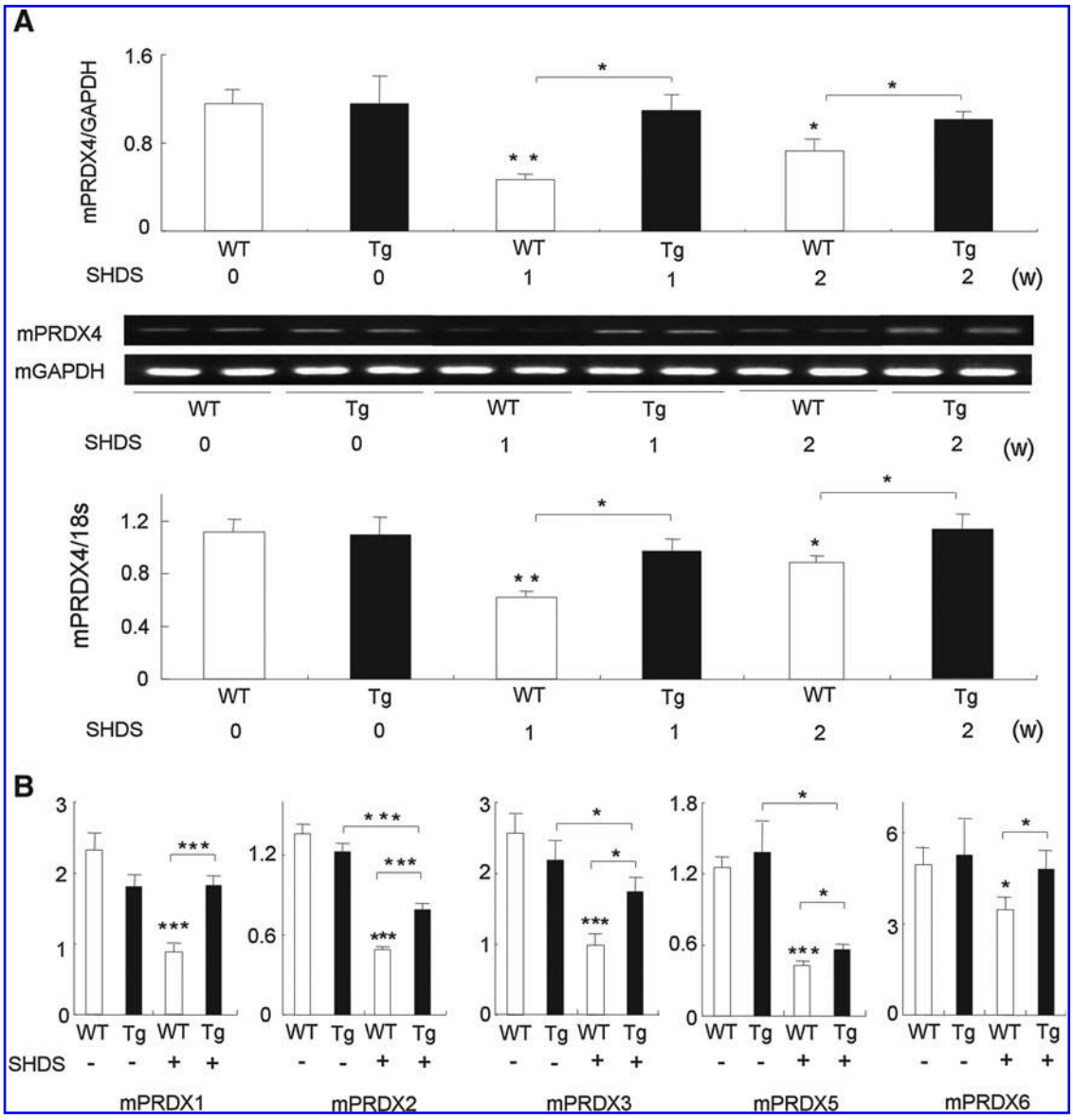

FIG. 5. Expressions of mPRDXs in WT and Tg pancreas. (**A**) RT- and real time-PCR demonstrated that the expression of mPRDX4 was not significantly different between WT and Tg mice pancreas under basal conditions at 0 wk. However, this expression was significantly higher in Tg than that in WT mice at 1 and 2 wk after SHDS-injection. Additionally, mPRDX4 level was markedly decreased in WT pancreas after SHDS-injection compared with untreated mice but this change was not observed in Tg pancreas. (**B**) In real-time PCR, the expression of various mPRDXs including PRDX 2, 3, and 5 was significantly downregulated in WT and Tg pancreas after SHDS-injection compared with nontreated mice, but mPRDX1 and 6 levels decreased only in WT mice. Also, these genes demonstrated significantly higher levels in Tg than those in WT mice after SHDS-injection. $*p < 0.05$, $**p < 0.001$, $***p < 0.0001$.

areas, percentage of insulin-positive cells, morphological appearances of islets, whole-body glucose homeostasis, or insulin resistance under basal conditions (Fig. 2). Besides, from a recent paper using PRDX4 knockout mice ($PRDX4^{-/y}$), whose spermatogenic cells were more susceptible to apoptosis via oxidative damage than those of wild-type $PRDX4^{+/y}$ male mice, PRDX4 protein in $PRDX4^{+/y}$ male mice was present in nearly all tissues with much higher levels found in testis and pancreas (16). These findings were similar to our results obtained by Western blotting and immunohistochemical analysis (Fig. 1 and Supplemental Fig. 2), although no morphological or biochemical difference was seen between the testes of our two groups of mice (data not shown).

After SHDS injection, WT mice showed a dramatic increase in blood glucose, a decrease in blood insulin levels, and a delay of glucose clearance. This damage to glucose/insulin metabolism should be attributed to disruption of pancreatic islets by SHDS. Tg mice, however, had significantly less hyperglycemia and hypoinsulinemia, along with a much faster response on the glucose tolerance test compared with treated WT mice, even though there was no significant difference in insulin resistance (Fig. 3). MLDS-induced diabetes models were performed at the same time, which is also well known to

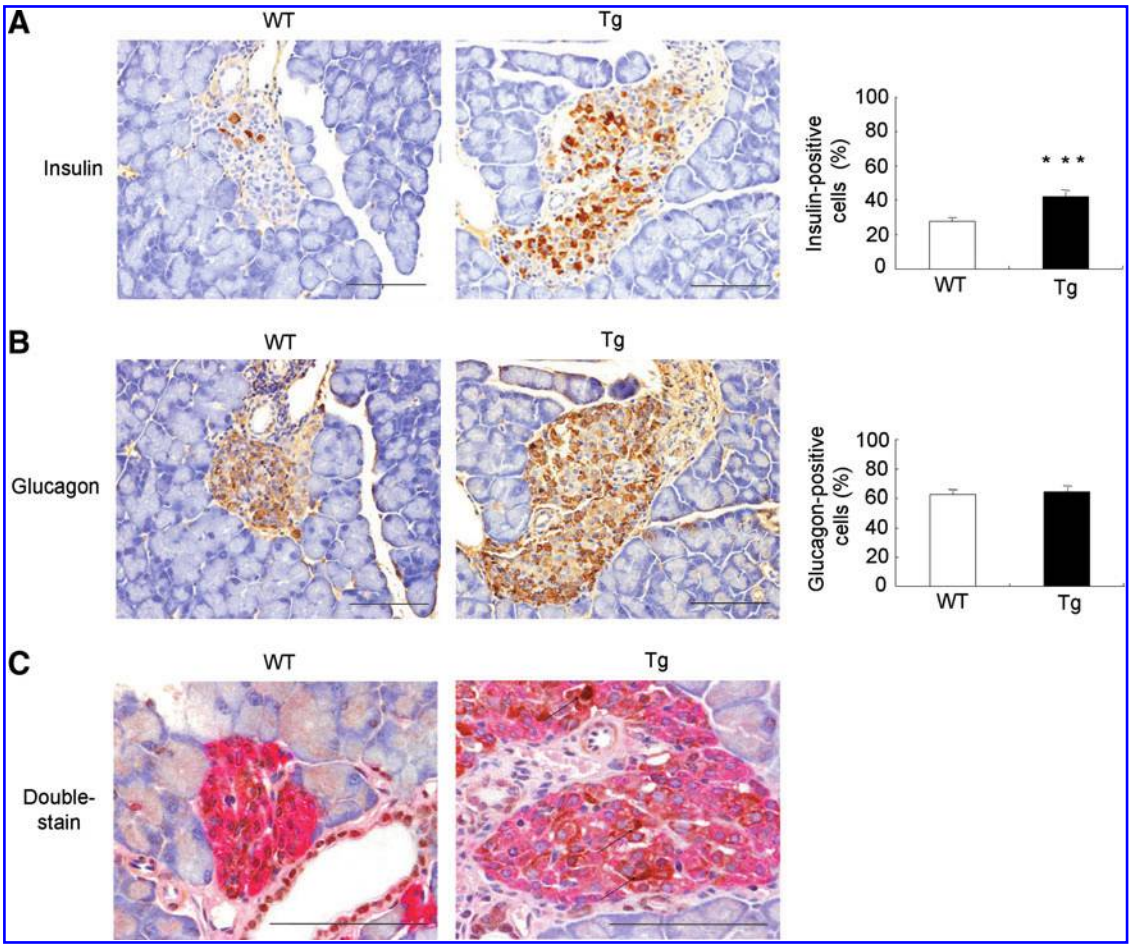

FIG. 6. Immunohistochemical analysis on WT and Tg pancreas 2 wk after SHDS-injection. (**A**) The percentage of insulin-positive β-cells per islet was significantly higher in Tg ($41.8 \pm 2.5\%$) compared with WT mice ($27.8 \pm 1.5\%$). (**B**) The percentage of glucagon-positive cells was not significantly different between the two groups (WT $63.0 \pm 1.6\%$ vs. Tg $64.6 \pm 1.5\%$). (**C**) In double immunostaining, both insulin- (*brown*) and glucagon- (*red*) positive cells were detected only in Tg islets (*arrows*). (**A**) and (**B**) 200X, (**C**) 400X, *Bar* = 100 μm. $^{***}p < 0.0001$. (For interpretation of the references to color in this figure legend, the reader is referred to the web version of this article at www.liebertonline.com/ars).

be a good model of T1DM. However, we could not demonstrate any more drastic or significant results including glucose levels, islet area alterations, or insulin-positive β-cells per islet between Tg and WT mice in MLDS models (Supplemental Fig. 3), compared with those induced by SHDS (Figs. 3, 4, and 6). Although this discrepancy between the two models cannot be further explained, SHDS models may be a more appropriate choice to study the *in vivo* function of PRDX4 compared with MLDS under the condition of PRDX4 overexpression.

Morphological observation showed that SHDS caused a serious injury to islet areas that were dramatically diminished in animals 1 or 2 wk after the injection. However, compared with WT mice, Tg mice revealed a resistance to injury and an accelerated reconstruction of the islets 2 wk after SHDS-injection, along with maintaining a high level of not only hPRDX4 (Fig. 4) but also endogenous mPRDXs expression including mPRDX4 (Fig. 5). This morphologic observation was in parallel with the above biological results. Therefore, these data indicated that overexpression of hPRDX4 in Tg mice protected against critical injury to islets by SHDS together with more resistant or less vulnerable endogenous mPRDXs expression, reminiscent of a cascade of PRDX family. This expression pattern restored the damage of glucose/insulin metabolism and amelioration of injured islets as observed in WT mice.

T1DM is primarily a T-cell-mediated disease termed 'insulitis' (4, 8, 24, 31, 33). Previous reports have shown that diabetes does not develop in non-obese diabetic mice that are genetically athymic or T lymphopenic (24). SHDS-injury causes a specific disruption of β-cells, an increase in the number of T-cells infiltrating into islets, and obstacles of insulin synthesis. Consequently, an inflammatory response takes place. Apoptosis is the main cause of selective β-cell death at the onset of T1DM, which is typically caused by an autoimmune assault against β-cells with infiltration of mononuclear cells (8, 24). Mechanisms of apoptosis involve direct T-cell cytotoxicity-, inflammatory factor-, and ROS-induced processes in insulitis (1, 2, 4, 8, 24, 28). In our experiments, the number of CD3-positive T-cells was increased in islets injured by SHDS, but the number of Mac-2-positive macrophages was not, indicating that the inflammatory response in this insulitis is attributed to increased infiltrating CD3-positive T-cells (Fig. 10). Therefore, the suppression of CD3-positive T-cell infiltration, but not of Mac-2-positive

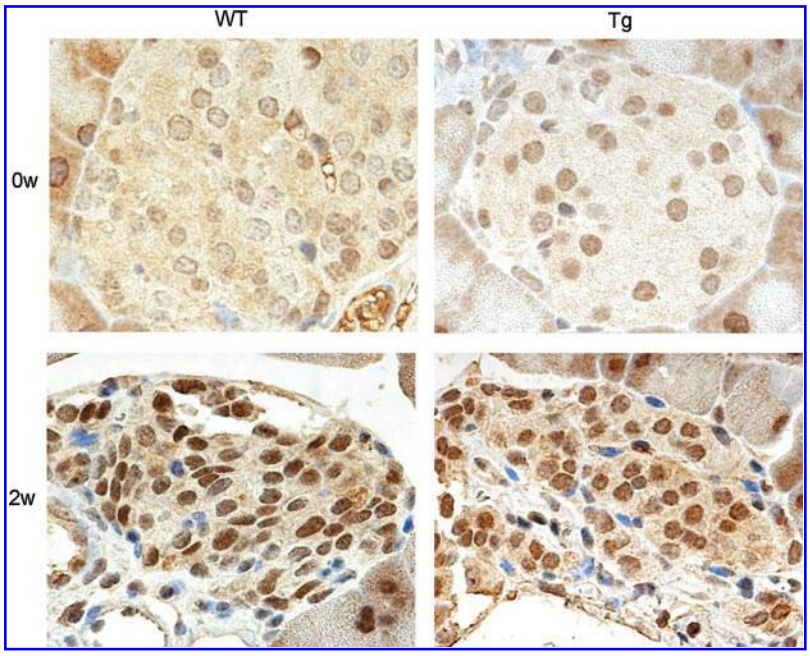

FIG. 7. Immunohistochemical expression of 8-OHdG in WT and Tg pancreas. The expression of 8-OHdG was very weak in untreated mice islets. However, at 2 wk after SHDS-injection, the expression was significantly increased in the pancreas of both groups. Additionally, 8-OHdG expression was significantly suppressed in Tg mice as compared with that in WT mice. 600X. (For interpretation of the references to color in this figure legend, the reader is referred to the web version of this article at www.liebertonline.com/ars).

macrophages, in Tg mice has a special implication in this model. These results show that hPRDX4 can suppress an infiltration of CD3-positive T lymphocytes.

In the regard to apoptosis, activated cytotoxic T-cells produce an inflammatory cytokine and release cytotoxic molecules including granzyme B or perforin. The consequence is that these cytokines can upregulate Fas expression on β-cells, thereby facilitating cell recognition via Fas/Fas ligand, activate the β-cell gene networks under the control of the transcription factors NFκ-B and STAT-1, and induce ROS, iNOS, and NO production, exacerbating apoptosis via caspase activation (1, 2, 13, 20, 24, 28). Indeed, we demonstrated that the expression of many inflammatory factors was significantly stimulated in WT mice after SHDS-induction. Conversely, such inflammatory signaling was significantly downregulated in Tg pancreas compared with those of WT pancreas (Fig. 8). As also shown in our data, particularly and classically, IL-1β has a more pronounced pro-apoptotic effect than others in β-cells, and some reports have demonstrated that *in vitro* exposure of β-cells to IL-1β or to IL-1β + IFN-γ

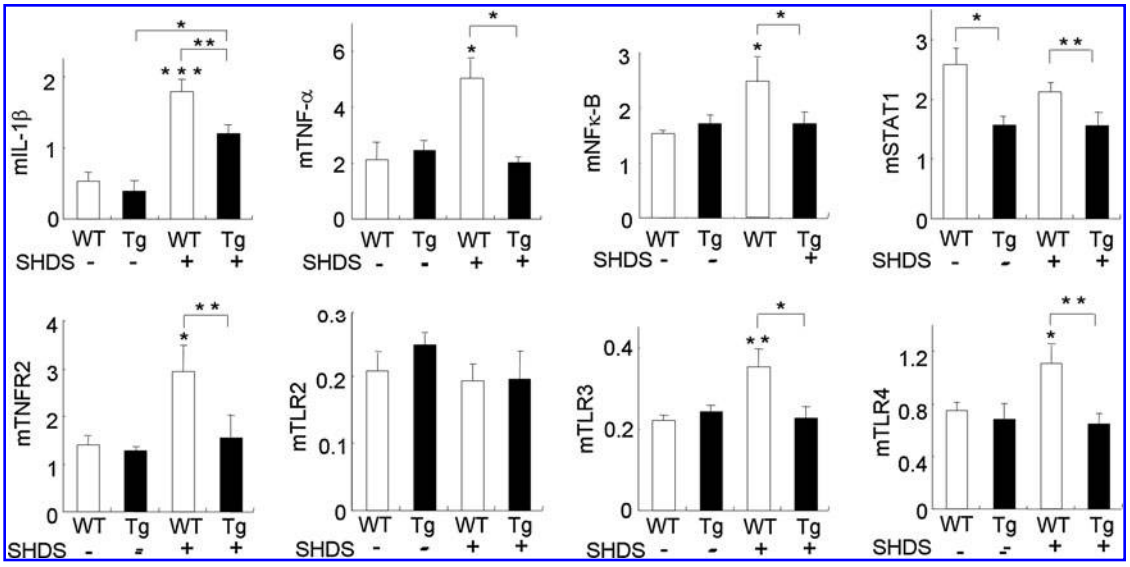

FIG. 8. Analysis of inflammatory signaling and tissue remodeling in WT and Tg pancreas by real-time PCR. Results demonstrated that various genes including IL-1β, TNF-α, NFκ-B, TNFR2, and TLR3/4 were markedly increased in WT mice 2 wk after SHDS-injection compared with untreated WT and treated Tg mice. However, the expression of these factors did not increase in Tg mice expect for IL-1β compared with the untreated Tg mice. The expression of STAT1 was significantly downregulated in Tg mice compared with both treated and untreated mice. A change in the expression of TLR2 was not detected. *$p < 0.05$, **$p < 0.001$, ***$p < 0.0001$.

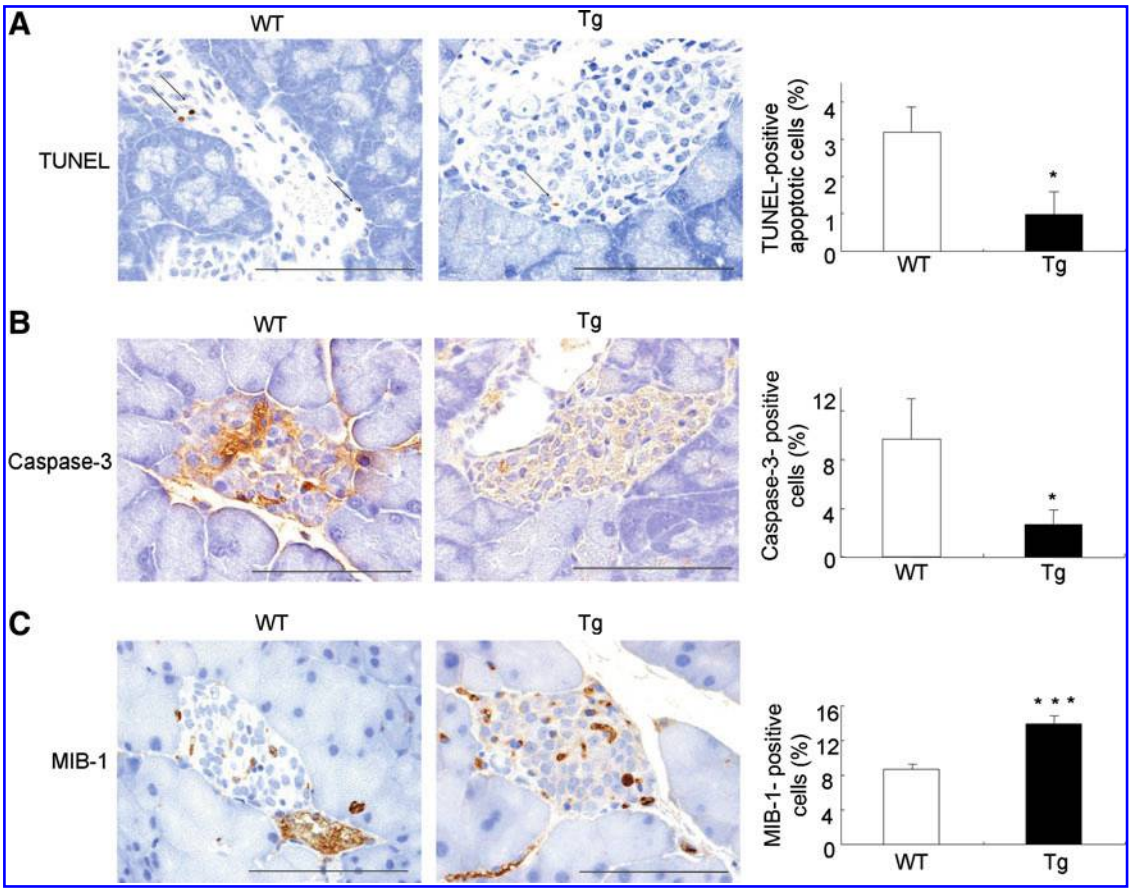

FIG. 9. Apoptosis and proliferation of β-cells in WT and Tg islets 1 wk after SHDS-injection. (**A**) In TUNEL staining, the percentage of TUNEL-positive apoptotic β-cells (*arrows*) per islet was significantly lower in Tg ($1.0 \pm 0.6\%$) than that of WT mice ($3.2 \pm 0.7\%$). (**B**) The percentage of caspase-3-positive cells was significantly decreased in Tg ($2.7 \pm 1.2\%$) compared with that of WT mice ($9.7 \pm 3.2\%$). (**C**) The percentage of MIB-1-positive cells was significantly increased in Tg ($13.9 \pm 0.9\%$) islet compared with that of WT mice ($8.7 \pm 0.6\%$). (**A, B**, and **C**) 400X, *Bar* = 100 μm. $^{*}p < 0.05$, $^{***}p < 0.0001$.

causes elevated proinsulin/insulin levels and a preferential loss of first-phase insulin secretion in response to glucose, which are very likely in diabetic patients (27). Besides, the significantly suppressed STAT-1 expression in Tg pancreas was interestingly noted not only in the treated but also in the untreated basal state (Fig. 8), unlike other inflammatory signaling and tissue remodeling genes. These results indicate that, particularly under the condition of PRDX4 overexpression, this transcription factor STAT-1 might play a critical role in SHDS-induced diabetes from initiation to progression, more recently described similar discussion by other groups (21). Furthermore, it is suggested that PRDX4 might have a close relationship with STAT-1.

It has been also reported that pancreatic islets have a markedly low antioxidative defense status and unusual susceptibility to ROS that cause apoptosis of β-cells in insulitis (2, 4, 9, 10, 12, 28). Since β-cell protective effects by PRDX4 may include ameliorating islet mass destruction with an accompanying significant decrease of inflammatory signaling in addition to suppression of CD3-positive T-cell infiltrate, hPRDX4 function should be implicated in the avoidance of β-cell apoptosis in Tg mice. Additionally, the expression of 8-OHdG, as an oxidative stress marker (15, 23), was much higher in WT and Tg islets after SHDS-injection than before treatment in immunohistochemistry (Fig. 7), supporting the premise that activated ROS production is not only induced by upregulated cytokines from stimulated T-cells, but also is derived from β-cells themselves in increased glucose concentration (12) in this diabetes model. At 2 wk, expression in Tg was borderline (in)significantly suppressed, as compared with that in WT mice. These results strongly suggest that hPRDX4 plays a protective role against injury by inhibiting cytotoxic T-cell infiltration as well as by preventing β-cell-derived ROS generation or scavenging of the generated ROS, particularly the extracellular pool of ROS. Compared with those of WT, the downregulated findings of TUNEL and caspase-3 activation in Tg islets verified (Fig. 9) and support these suggestions.

TLRs belong to a superfamily that shares signaling components with IL-1 receptors and are essential for the recognition of pathogen-associated molecular patterns including conserved microbial components (22). TLR 2, 3, and 4 are strongly expressed in normal murine pancreatic islets (34–36), and activation of TLR3 signaling plays an important role in the viral replicative intermediate double-stranded RNA (dsRNA)-induced insulitis and β-cell apoptosis (29, 36). Therefore, our results showing a significantly higher or lower expression of TLR3 and 4 in WT or Tg pancreas (Fig. 8),

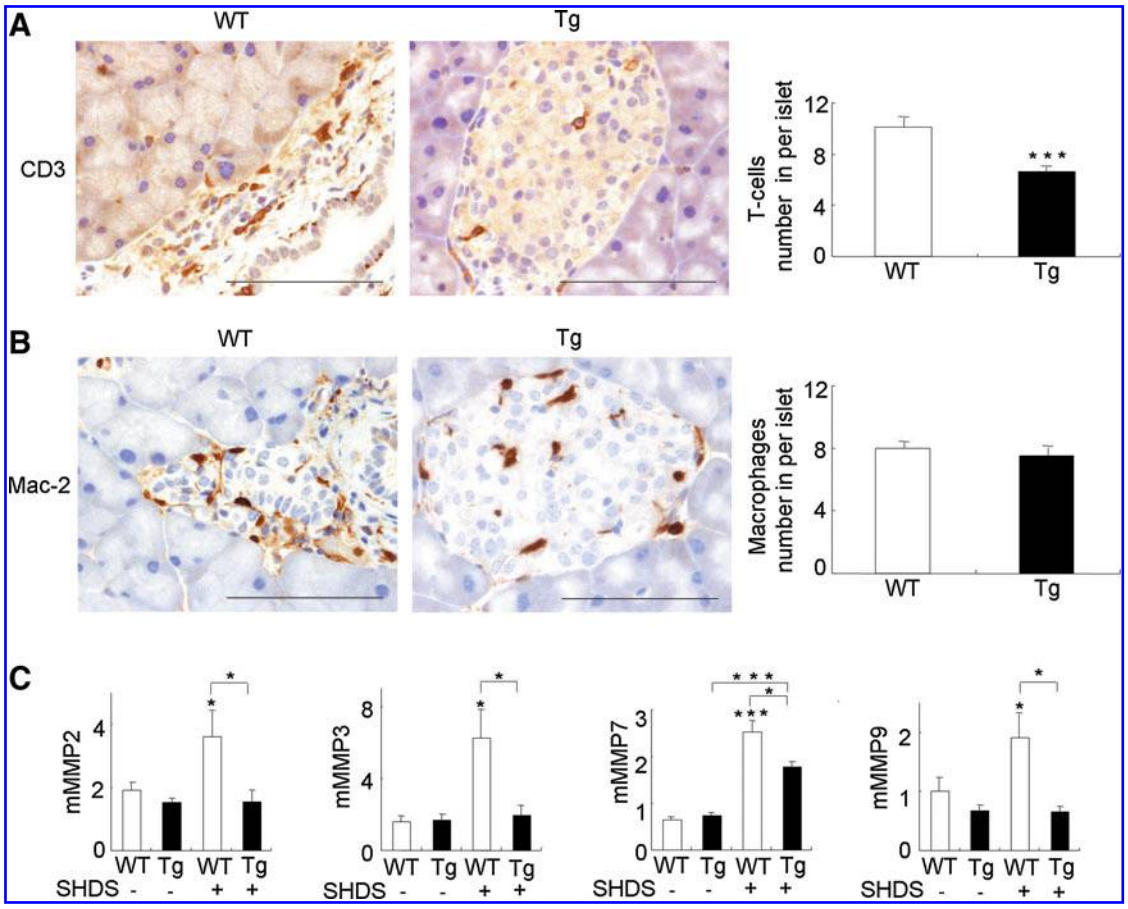

FIG. 10. Insulitis in islets and MMPs analysis in WT and Tg pancreas 2 wk after SHDS-treatment. (**A**) The number of CD3-positive infiltrating T-lymphocytes per islet was significantly smaller in Tg (6.6 ± 0.4) than that of WT mice (10.1 ± 0.7). (**B**) Mac-2 analysis for infiltrating macrophages demonstrated no difference between WT and Tg islets (WT 8.0 ± 0.4 vs. Tg 7.5 ± 0.5). (**C**) The expression of MMP2, 3, 7, and 9 was significantly upregulated in WT pancreas compared with those of Tg mice 2 wk after SHDS-injection and untreated WT mice. Only MMP7 expression was higher in Tg mice than that of untreated mice. (**A**) and (**B**) 400X, $Bar = 100\,\mu$m. $^{*}p < 0.05$, $^{***}p < 0.0001$. (For interpretation of the references to color in this figure legend, the reader is referred to the web version of this article at www.liebertonline.com/ars).

respectively, may not correspond to a viral infection but to the expression of proinflammatory cytokines in these animals.

In the current study, we found new pathological findings that the proportion of glucagon-positive cells in both of Tg and WT is markedly increased by about 64% after SHDS-induced islet destruction (Fig. 6B). Consequently, proliferating glucagon-positive cells became a predominant component of islets. That result suggested that the replication of glucagon-positive cells compensated for the significantly decreasing numbers of β-cells caused by insulitis and apoptosis. In addition, the islet replication rate was significantly higher in Tg than in WT pancreas based on the MIB-1 immunohistochemical results after SHDS-injection (Fig. 9C). Interestingly, replicating β-cells in Tg islets were partially overlapping with replicating α-cells, which was supported by the results that adding the proportion of α- and β-cell from Tg tissue after islet destruction exceeds more than 100%. In direct contract, a proportion of less than 100% was found in WT islets (Figs. 6A and 6B). These results indicated that the regenerative and neogenetic islet cells may be immature and pluripotent, and as a result, both glucagon and insulin are immunoreactive with one part of many replicating cells in Tg mice (Fig. 6C). The current study has demonstrated that a rapid course of islet hyperplasia after streptozotocin-induced injury depends on endogenous stem/progenitor cell conversion into β-cells, or α- and subsequently into β-cells (5, 38). The expression of hPRDX4 may accelerate replication of pluripotent cells to repair and remodel islets.

Members of the MMP family, which cleave various extracellular matrix macromolecules (ECM), possess a broad range of pathophysiological activities including regulation of cell replication and/or apoptosis and are associated with inflammatory responses and cytokine production (32, 39). ECM are components of pancreatic islets, and their turnover is critical for insular development (6, 7, 17). A recent report indicates that tissue inhibitors of the metalloproteinase (TIMP)-1 gene, one representative of the MMP-inhibitor family, can be a potential target to prevent T1DM, based on the results that overexpression of TIMP-1 in β-cells accelerates the replication of destructive β-cells and counteracts T1DM (17). Our results showed that the lower levels of insulitis in Tg pancreas are associated with more significantly suppressed expression not only of MMP-9, but also those of other MMPs such as MMP-2, -3 and -7 compared with those of WT mice (Fig. 10C), which

indicate a correlation between MMPs in the inflammatory signaling cascade in insulitis. Our results indicate that PRDX4 modulates islet remodeling of the islets with accompanying replication of stem/progenitor cells.

In conclusion, insulin-secreting β-cells in Tg islets are more significantly protective against SHDS-induced insulitis and apoptosis than those of WT. In addition, hPRDX4 was more likely to activate the proliferation of stem/progenitor cells to recover the population of β-cells in Tg islets. The mechanisms of PRDX4 in the suppression of apoptosis and stimulation of replication of stem/progenitor cells may involve scavenging increased ROS/oxidative stress and preventing inflammatory signaling activation, particularly of T-cell infiltrates. Considering the broad spectrum of substrates of PRDX4, all results obtained in our experiments may not be attributable only to the protection against oxidative stress-induced β-cell dysfunction. These observations indicate that hPRDX4 transgenic mice could become a useful animal model to study the relevance between oxidative stress and inflammation, and that a specific accelerator of PRDX4 might prove to be a potential therapeutic agent for ameliorating T1DM by suppressing oxidative damage and inflammatory cytokines throughout the course of the disease. PRDX4 may be pathophysiologically relevant to protection against diabetes in humans.

Acknowledgments

This work was supported in part by Grants-in-Aid for Scientific Research (19590413 and 20590416) from the Ministry of Education, Culture, Sports, Science, and Technology, Tokyo, Japan (to YS, KK, and AT).

Author Disclosure Statement

No competing financial interests exist.

References

1. Andersen NA, Larsen CM, and Mandrup–Poulsen T. TNFα and IFNγ potentiate IL-1β induced mitogen activated protein kinase activity in rat pancreatic islets of Langerhans. *Diabetologia* 43: 1389–1396, 2000.
2. Chen H, Li X, and Epstein PN. MnSOD and catalase transgenes demonstrate that protection of islets from oxidative stress does not alter cytokine toxicity. *Diabetes* 54: 1437–1446, 2005.
3. Choi MH, Lee IK, Kim GW, Kim BU, Han YH, Yu DY, Park HS, Kim KY, Lee JS, Choi C, Bae YS, Lee BI, Rhee SG, and Kang SW. Regulation of PDGF signalling and vascular remodelling by peroxiredoxin II. *Nature* 435: 347–353, 2005.
4. Cnop M, Welsh N, Jonas JC, Jörns A, Lenzen S, and Eizirik DL. Mechanisms of pancreatic beta-cell death in type 1 and type 2 diabetes: Many differences, few similarities. *Diabetes* 54: S97–107, 2005.
5. Collombat P, Xu X, Ravassard P, Sosa–Pineda B, Dussaud S, Billestrup N, Madsen OD, Serup P, Heimberg H, and Mansouri A. The ectopic expression of *Pax*4 in the mouse pancreas converts progenitor cells into α and subsequently β-cells. *Cell* 138: 449–462, 2009.
6. Descamps FJ, Martens E, Ballaux F, Geboes K, and Opdenakker G. *In vivo* activation of gelatinase B/MMP-9 by trypsin in acute pancreatitis is a permissive factor in streptozotocin-induced diabetes. *J Pathol* 204: 555–561, 2004.
7. Descamps FJ, Van den Steen PE, Martens E, Ballaux F, Geboes K, and Opdenakker G. Gelatinase B is diabetogenic in acute and chronic pancreatitis by cleaving insulin. *FASEB J* 17: 887–889, 2003.
8. Donath MY, Storling J, Maedler K, and Mandrup–Poulsen T. Inflammatory mediators and islet β-cell failure: a link between type 1 and type 2 diabetes. *J Mol Med* 81: 455–470, 2003.
9. Evans JL, Goldfine ID, Maddux BA, and Grodsky GM. Are oxidative stress-activated signaling pathways mediators of insulin resistance and β-cell dysfunction? *Diabetes* 52: 1–8, 2003.
10. Fridlyand LE and Philipson LH. Does the glucose-dependent insulin secretion mechanism itself cause oxidative stress in pancreatic β-cells? *Diabetes* 53: 1942–1948, 2004.
11. Giguere P, Turcotte ME, Hamelin E, Parent A, Brisson J, Laroche G, Labrecque P, Dupuis G, and Parent JL. Peroxiredoxin-4 interacts with and regulates the thromboxane A_2 receptor. *FEBS Lett* 581: 3863–3868, 2007.
12. Gurgul E, Lortz S, Tiedge M, Jörns A, and Lenzen S. Mitochondrial catalase overexpression protects insulin-producing cells against toxicity of reactive oxygen species and proinflammatory cytokines. *Diabetes* 53: 2271–2280, 2004.
13. Gysemans CA, Ladrière L, Callewaert H, Rasschaert J, Flamez D, Levy DE, Matthys P, Eizirik DL, and Mathieu C. Disruption of the γ-interferon signaling pathway at the level of signal transducer and activator of transcription-1 prevents immune destruction of β-cells. *Diabetes* 54: 2396–2403, 2005.
14. Hong CC, Kume T, and Peterson RT. Role of crosstalk between phosphatidylinositol 3-kinase and extracellular signal-regulated kinase/mitogen-activated protein kinase pathways in artery-vein specification. *Circ Res* 103: 573–579, 2008.
15. Ihara Y, Toyokuni S, Uchida K, Odaka H, Tanaka T, Ikeda H, Hiai H, Seino Y, and Yamada Y. Hyperglycemia causes oxidative stress in pancreatic β-cells of GK rats, a model of type 2 diabetes. *Diabetes* 48: 927–932, 1999.
16. Iuchi Y, Okada f, Tsunoda S, Kibe N, Shirasawa N, Ikawa M, Okabe M, Ikeda Y, and Fujii J. Peroxiredoxin 4 knockout results in elevated spermatogenic cell death via oxidative stress. *Biochem J* 419: 149–158, 2009.
17. Jiang H, Zhu H, Chen X, Peng Y, Wang J, Liu F, Shi S, Fu B, Lu Y, Hong Q, Feng Z, Hou K, Sun X, Cai G, Zhang X, and Xie Y. TIMP-1 transgenic mice recover from diabetes induced by multiple low-dose streptozotocin. *Diabetes* 56: 49–56, 2007.
18. Jin DY, Chae HZ, Rhee SG, and Jeang KT. Regulatory role for a novel human thioredoxin peroxidase in NF-κB activation. *J Biol Chem* 272: 30952–30961, 1997.
19. Kang SW, Rhee SG, Chang TS, Jeong W, and Choi MH. 2-Cys peroxiredoxin function in intracellular signal transduction: Therapeutic implications. *Trends Mol Med* 11: 571–578, 2005.
20. Karlsen AE, Pavlovic D, Nielsen K, Jensen J, Andersen HU, Pociot F, Mandrup–Poulsen T, Eizirik DL, and Nerup J. Interferon-γ induces interleukin-1 converting enzyme expression in pancreatic islets by an interferon regulatory factor-1-dependent mechanism. *J Clin Endocrinol Metab* 85: 830–836, 2000.
21. Kim S, Kim HS, Chung KW, Oh SH, Yun JW, Im SH, Lee MK, Kim KW, and Lee MS. Essential role for signal transducer and activator of transcription-1 in pancreatic β-cell

death and autoimmune type 1 diabetes of nonobese diabetic mice. *Diabetes* 56: 2561–2568, 2007.
22. Krishnan J, Selvarajoo K, Tsuchiya M, Lee G, and Choi S. Toll-like receptor signal transduction. *Exp Mol Med* 39: 421–438, 2007.
23. Ku YP, Jin M, Kim KH, Ahn YJ, Yoon SP, You HJ, and Chang IY. Immunolocalization of 8-OHdG and OGG1 in pancreatic islets of streptozotocin-induced diabetic rats. *Acta Histochem* 111: 138–144, 2009.
24. Mathis D, Vence L, and Benoist C. β-Cell death during progression to diabetes. *Nature* 414: 792–798, 2001.
25. Matsumoto A, Okado A, Fujii T, J Fujii J, Egashira M, Niikawa N, and Taniguchi N. Cloning of the peroxiredoxin gene family in rats and characterization of the fourth member. *FEBS Lett* 443: 246–250, 1999.
26. Neumann CA, Krause DS, Carman CV, Das S, Dubey DP, Abraham JL, Bronson RT, Fujiwara Y, Orkin SH, and Van Etten RA. Essential role for the peroxiredoxin Prdx1 in erythrocyte antioxidant defence and tumour suppression. *Nature* 424: 561–565, 2003.
27. Ohara-Imaizumi M, Cardozo AK, Kikuta T, Eizirik DL, and Nagamatsu S. The cytokine interleukin-1beta reduces the docking and fusion of insulin granules in pancreatic beta-cells, preferentially decreasing the first phase of exocytosis. *J Biol Chem* 279: 41271–41274, 2004.
28. Ortis F, Pirot P, Naamane N, Kreins AY, Rasscheart J, Moore F, Theatre E, Verhaeghe C, Magnusson NE, Chariot A, Orntoft TF, and Eizirik DL. Induction of nuclear factor-κB and its downstream genes by TNF-α and IL-1β has a pro-apoptotic role in pancreatic beta cells. *Diabetologia* 51: 1213–1225, 2008.
29. Rasschaert J, Ladrière L, Urbain M, Dogusan Z, Katabua B, Sato S, Akira S, Gysemans C, Mathieu C, and Eizirik DL. Toll-like receptor 3 and STAT-1 contribute to double-stranded RNA+ interferon-γ-induced apoptosis in primary pancreatic β-cells. *J Biol Chem* 280: 33984–33991, 2005.
30. Rhee SG, Chae HZ, and Kim K. Peroxiredoxins: A historical overview and speculative preview of novel mechanisms and emerging concepts in cell signaling. *Free Radic Biol Med* 38: 1543–1552, 2005.
31. Riboulet–Chavey A, Diraison F, Siew LK, Wong FS, and Rutter GA. Inhibition of AMP-activated protein kinase protects pancreatic β-cells from cytokine-mediated apoptosis and CD8+ T-cell-induced cytotoxicity. *Diabetes* 57: 415–423, 2008.
32. Takagishi T, Sasaguri Y, Nakano R, Arima N, Tanimoto A, Fukui H, and Morimatsu M. Expression of the histamine H1 receptor gene in relation to atherosclerosis. *Am J Pathol* 146: 981–988, 1995.
33. Tisch R and McDevitt H. Insulin-dependent diabetes mellitus. *Cell* 85: 291–297, 1996.
34. Triantafilou K and Triantafilou M. Coxsackievirus B4-induced cytokine production in pancreatic cells is mediated through toll-like receptor 4. *J Virol* 78: 11313–11320, 2004.
35. Vives–Pi M, Somoza N, Fernandez-Alvarez J, Vargas F, Caro P, Alba A, Gomis R, Labeta MO, and Pujol–Borrell R. Evidence of expression of endotoxin receptors CD14, toll-like receptors TLR4 and TLR2 and associated molecule MD-2 and of sensitivity to endotoxin (LPS) in islet beta cells. *Clin Exp Immunol* 133: 208–218, 2003.
36. Wen L, Peng J, Li Z, and Wong FS. The effect of innate immunity on autoimmune diabetes and the expression of Toll-like receptors on pancreatic islets. *J Immunol* 172: 3173–3180, 2004.
37. Wong CM, Chun AC, Kok KH, Zhou Y, Fung PC, Kung HF, Jeang KT, and Jin DY. Characterization of human and mouse peroxiredoxin IV: Evidence for inhibition by Prx-IV of epidermal growth factor and p53-induced reactive oxygen species. Antioxid Redox Signal 2: 507–518, 2000.
39. Xu X, D'Hoker J, Stange G, Bonne S, Leu DN, Xiao X, Casteele MVD, Mellitzer G, Ling Z, Pipeleers D, Bouwens L, Scharfmann R, Gradwohl G, and Heimberg H. β cells can be generated from endogenous progenitors in injured adult mouse pancreas. *Cell* 132: 197–207, 2008.
40. Yamada S, Wang KY, Tanimoto A, Fan JL, Shimajiri S, Kitajima S, Morimoto M, Tsutsui M, Watanabe T, Yasumoto K, and Sasaguri Y. Matrix metalloproteinase 12 accelerates the initiation of atherosclerosis and stimulates the progression of fatty streaks to fibrous plaques in transgenic rabbits. *Am J Pathol* 172: 1419–1429, 2008.

Address correspondence to:
Yasuyuki Sasaguri, M.D., Ph.D.
Department of Pathology and Cell Biology
School of Medicine
University of Occupational and Environmental Health
1-1 Iseigaoka, Yahatanishi-ku
Kitakyushu 807-8555
Japan

E-mail: yasu3219@med.uoeh-u.ac.jp

Date of first submission to ARS Central, February 4, 2010; date of final revised submission, April 19, 2010; date of acceptance, May 1, 2010.

Abbreviations Used

8-OHdG = 8-hydroxy-2′-deoxyguanosine
BGHPA = bovine growth hormone polyadenylation
CMV = cytomegalovirus
ECM = extracellular matrix macromolecules
h = hours
H&E = hematoxylin and eosin
H_2O_2 = hydrogen peroxide
IFN-γ = interferon-γ
IL-1β = interleukin-1β
iNOS = inducible nitric oxide synthase
MLDS = multiple low dose of streptozotocin
MMPs = matrix metalloproteinases
NFκ-B = nuclear factor κ-B
NO = nitric oxide
O_2^- = superoxide anion
PRDX = peroxiredoxin
ROS = reactive oxygen species
RT-PCR = reverse transcriptase-polymerase chain reaction
SHDS = single high dose of streptozotocin
STAT-1 = signal transducer and activator of transcription-1
T1DM = type 1 diabetes mellitus
Tg = transgenic
TIMP-1 = tissue inhibitors of the metalloproteinase-1
TLRs = Toll-like receptors
TNF-α = tumor necrosis factor-α
wk = weeks
WT = wild-type

This article has been cited by:

1. Xin Guo , Sohsuke Yamada , Akihide Tanimoto , Yan Ding , Ke-Yong Wang , Shohei Shimajiri , Yoshitaka Murata , Satoshi Kimura , Takashi Tasaki , Atsunori Nabeshima , Teruo Watanabe , Kimitoshi Kohno , Yasuyuki Sasaguri . 2012. Overexpression of Peroxiredoxin 4 Attenuates Atherosclerosis in Apolipoprotein E Knockout Mice. *Antioxidants & Redox Signaling* **17**:10, 1362-1375. [Abstract] [Full Text HTML] [Full Text PDF] [Full Text PDF with Links] [Supplemental material]
2. G. Drews, M. Düfer. 2012. Role of KATP channels in #-cell resistance to oxidative stress. *Diabetes, Obesity and Metabolism* **14**, 120-128. [CrossRef]
3. Tatsuya Oba, Ryosuke Tatsunami, Keisuke Sato, Kyohei Takahashi, Zhihui Hao, Yoshiko Tampo. 2012. Methylglyoxal has deleterious effects on thioredoxin in human aortic endothelial cells. *Environmental Toxicology and Pharmacology* **34**:2, 117-126. [CrossRef]
4. JennaLynn Styskal, Holly Van Remmen, Arlan Richardson, Adam B. Salmon. 2012. Oxidative stress and diabetes: What can we learn about insulin resistance from antioxidant mutant mouse models?. *Free Radical Biology and Medicine* **52**:1, 46-58. [CrossRef]
5. Anke Di, Xiao-Pei Gao, Feng Qian, Takeshi Kawamura, Jin Han, Claudie Hecquet, Richard D Ye, Stephen M Vogel, Asrar B Malik. 2011. The redox-sensitive cation channel TRPM2 modulates phagocyte ROS production and inflammation. *Nature Immunology* . [CrossRef]
6. LYNN PETUKHOVA, RITA M. CABRAL, JULIAN MACKAY-WIGGAN, RAPHAEL CLYNES, ANGELA M. CHRISTIANO. 2011. The genetics of alopecia areata: What's new and how will it help our patients?. *Dermatologic Therapy* **24**:3, 326-336. [CrossRef]
7. Melinda T. Coughlan, Josephine M. Forbes. 2011. Temporal Increases in Urinary Carboxymethyllysine Correlate with Albuminuria Development in Diabetes. *American Journal of Nephrology* **34**:1, 9-17. [CrossRef]